IOP Conf. Series: Materials Science and Engineering **232** (2017) 012002 doi:10.1088/1757-899X/232/1/012002

Thermal and Fluid Mechanical Investigation of an Internally Cooled Piston Rod

K Klotsche[1], C Thomas[1] and U Hesse[1]

[1] Technische Universität Dresden, Institute of Power Engineering, Bitzer Chair of Refrigeration, Cryogenics and Compressor Technology, 01062 Dresden, Germany

konrad.klotsche@tu-dresden.de

Abstract. The Internal Cooling of Reciprocating Compressor Parts (ICRC) is a promising technology to reduce the temperature of the thermally stressed piston and piston rod of process gas compressors. The underlying heat transport is based on the flow of a two-phase cooling medium that is contained in the hollow reciprocating assembly. The reciprocating motion forces the phases to mix, enabling an enhanced heat transfer.
In order to investigate this heat transfer, experimental results from a vertically reciprocating hollow rod are presented that show the influence of different liquid charges for different working temperatures. In addition, pressure sensors are used for a crank angle dependent analysis of the fluid mechanical processes inside the rod. The results serve to investigate the two-phase flow in terms of the velocity and distribution of the liquid and vapour phase for different liquid fractions.

1. Motivation

Thermodynamics and heat transfer play a key role during the compression process, particularly with regard to the energy and volumetric efficiency but also to the durability of sealing elements. The latter applies particularly to non-lubricated materials. Several studies[1,2,3] have addressed the effect of cooling on the abovementioned aspects and the actual potential was rated differently. However, the impact of compressor cooling depends on the specific compressor setup and especially on the realisation of the cooling concept. Thus, it is needed to be reassessed from case to case.

Heat is typically considered to be rejected from the outer cylinder parts either by a cooling system within the cylinder walls or by a cooled packing at the piston rod of crosshead-type piston compressors. In contrast, a novel cooling technique – the Internal Cooling of Reciprocating Compressor Parts (ICRC) – constitutes a promising and convenient possibility to reject heat through the reciprocating assembly. For this, a two-phase fluid contained inside the reciprocating assembly is intermixed by reciprocating motion, thus, transferring heat to the crosshead and finally rejecting it to the crank case oil.

Several experimental as well as theoretical investigations had been performed over the last years in order to gain more information about the potential heat transfer of the ICRC. It appeared that the heat transfer through the piston rod can be increased by a couple of orders of magnitude compared to solid designs. Those studies were mainly focused on the thermodynamic behaviour. For a deeper understanding of the occurring phenomena and for the pre-calculation of the heat transfer of the ICRC for a specific compressor configuration, improved knowledge about the two-phase flow of the contained fluid, *i. e.* the velocity and the distribution of the liquid and vapour phase is required. Therefore, based on the thermodynamic results and pressure measurements, a first insight into the fluid mechanical processes of the two-phase flow inside a vertical reciprocating hollow rod is provided. Furthermore, the

suitability of the cooling fluid used in previous studies[4] is reviewed for different filling amounts and particularly for varying temperatures.

2. Internal Cooling of Reciprocating Compressor Parts (ICRC)

The idea of an internal cooling of the reciprocating assembly of piston compressors dates back to 2007 as Quack and Nickl[5] had patented this concept. The following section provides an overview of the principle of operation and previous research.

2.1. Principle of operation

The ICRC aims at cooling of compressor components that are thermally stressed due to their direct contact with the working fluid and due to friction at the sealing gaps. For this purpose, a two-phase coolant is contained within the hollow reciprocating assembly, *e. g.* the piston and the piston rod, see Fig. 1. Owing to the reciprocating motion, both phases are generally intermixed and, in doing so, coolant flows back and forth between both ends of the cavity. Thereby, heat is absorbed from warmer parts, *e. g.* from the piston or from the packing area, transported through the reciprocating assembly and released at the colder oil-lubricated crosshead.

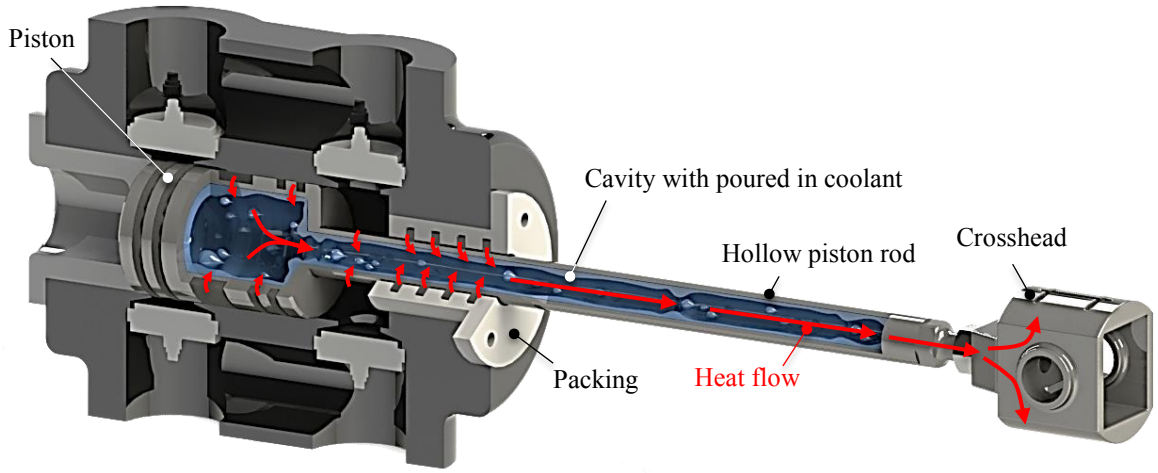

Figure 1. Design and principle of operation of the ICRC

Obviously, the temperature difference between the cylinder area and the crosshead as thermal drive is also present within a conventional solid design of the reciprocating components. But, the fundamental idea and main benefit of this cooling technology is to make use of the intensified fluid flow inside the cavity caused by the high-frequency reciprocating motion. This engenders a much lower thermal resistance of the reciprocating assembly, which results in an increased cooling effect for the cylinder area.

2.2. Previous research

Since the first reference of the ICRC idea, several experimental and theoretical studies were conducted, focusing at first on its feasibility and general applicability. Thomas[4] presented extensive results from both experimental and theoretical investigations which show the effectiveness of the internal cooling at three different test rigs, including a single-stage double-acting balanced-opposed compressor. In comparison to a solid piston rod, the implementation of an internally cooled piston rod had led to a reduction of the gas temperature inside the packing of up to 80 K.

In 2016 Klotsche *et al*[6] have shown the influence of the internal diameter on the heat transfer of a vertical configuration of the ICRC by means of experimental investigations. The axial heat flux could

be quantified by a subsequent numerical analysis in the range of 13 W/cm² to 30 W/cm². For the same (vertical) configuration and a similar manner, the effect of different potential coolants on the heat transfer was examined by Klotsche *et al*[7]. Additionally, for the most promising coolant the optimal filling amount could be found.

3. Experimental investigation

3.1. Test rig setup

For the experimental investigation of the heat transfer inside a reciprocating hollow rod a test rig is available at the Technische Universität Dresden (see Fig. 2). It comprises a vertically reciprocating hollow rod actuated by a crank drive that is driven by an electric motor. The stroke s is 100 mm and the length of the connecting rod l is 250 mm. The rod is mounted onto a temperature-controlled crosshead. This crosshead comprises a cooling duct connected to an external cooling circuit providing the entire heat to be rejected at the rod's lower end, *i. e.* the temperature at this location can be held constant for all operation points. At the upper end of the rod a cylindrically shaped electrical heater is installed to provide a precisely adjustable heat input. At the top the rod is closed by an end cap. All relevant components except the crosshead are insulated against the ambient environment to guide the majority of the heat input through the fluid. In order to connect any electrical signals to the measurement system and to guide the crosshead coolant from the test rig to the cooling unit of the laboratory, an energy chain is attached to the rod's cap.

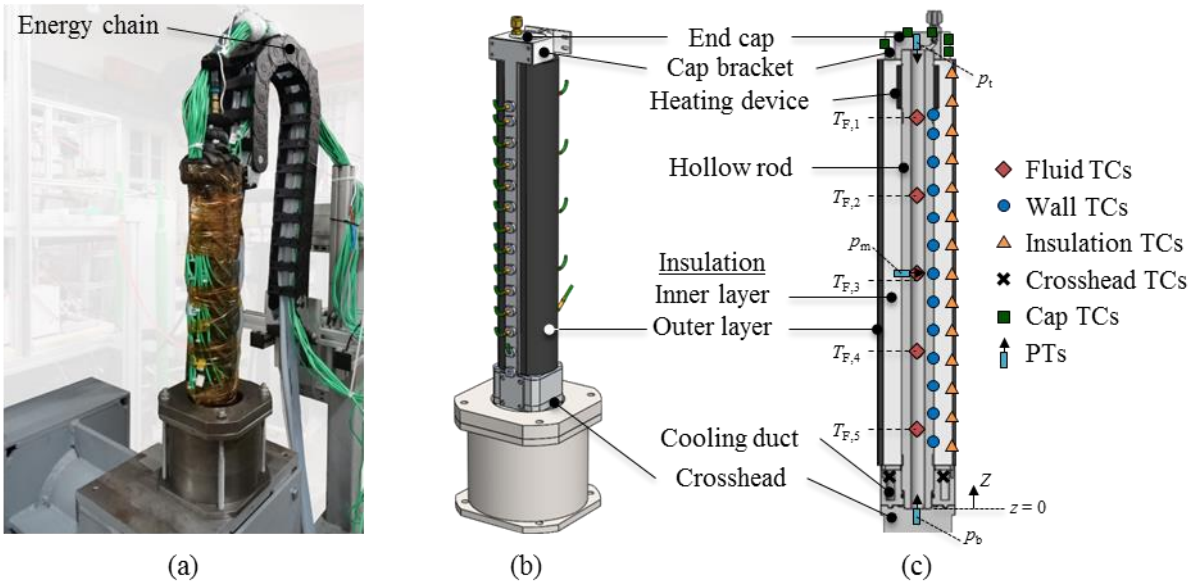

Figure 2. Setup of the test rig (a), CAD representation (b), and sectional view with installed thermocouples (TCs) and pressure transducers (PTs) with measuring direction (c)

To record the temperature field of all relevant components, 39 type K thermocouples (TCs) are installed whose signals are sampled at 1 Hz. Their locations can be seen in Fig. 2 (c). Five TCs ($T_{F,1}$…$T_{F,5}$) positioned inside the cavity are distributed along the rod's axis z measuring the fluid temperature. Thirteen temperature sensors are positioned 2 mm below the rod's external radial surface capturing the wall temperature. They are distributed along the z-axis similar to the fluid TCs. Additionally, two TCs are located at the rod's cap and 3 TCs at the lateral surface of the cap bracket as well as 2 TCs inside the cooling duct of the crosshead. The rod is equipped with two insulation layers. Fourteen TCs within the insulation layers measure the temperature along the rod's axis. As described in

a previous work[6] the cap, insulation and crosshead TCs can be used as boundary conditions for a simulation of the temperature field by the FEM program Ansys.

For the investigation of the dynamic fluid behaviour, 3 pressure transducer (PTs, Kulite XTEL-190) with a possible sampling frequency of up to 100 kHz are positioned at the upper and lower end face of the cavity as well as at medium height. The measuring direction of the PTs, which is perpendicular to the mounting wall, is depicted in Fig. 2. The high-frequency pressure signals are referenced to the position of the rod, *i. e.* bottom dead centre (BDC) and top dead centre (TDC), by a rotary angle sensor.

3.2. Measurement procedure

At first, the cavity, which is opened to ambient air, is filled by the coolant. Then the hollow rod is closed. This results in a coolant-air mixture at ambient conditions. Then the rotational speed is adjusted and the flow through the crosshead's cooling circuit as well as the power supply of the heater is switched on. After a transient period in which the temperatures are converging towards a steady-state, the subsequent interval is used to record the final temperatures which are averaged over 5 minutes. In this way, long term transient phenomena are excluded. In the quasi-stationary state, also the dynamic pressure measurements were conducted for 10 crank revolutions at a sampling rate of 50 kHz.

3.3. Measurement series

Previous studies[7] with a natural coolant showed that a liquid volume fraction ε of 30% exhibits the highest heat transfer rates in comparison to 10%, 20%, 40%, and 50%. It cannot be assumed that there is another optimum outside this range of liquid fractions. Therefore, this study, as a first step, is intended to investigate the heat transfer and the occurring temperatures for a finer division (5% steps) in the range of 20% to 40%.

Furthermore, it is known from the heat pipe literature[8] that the heat transfer capability for a certain cooling fluid – typically represented as Merit number – changes with temperature due to the change of fluid properties. In order to analyse whether the temperature affects the found optimum of the filling amount, different liquid fractions were tested with varying heat loads (0 W to 250 W in steps of 50 W).

For all shown measurements, the rotational speed n was set to 500 min^{-1} and the inlet temperature of the crosshead coolant T_C to 10 °C. All measurements were carried out under laboratory conditions ensuring the ambient temperature to be sufficiently constant over time. Hence, all (thermal) boundary conditions are consistent, except the heat input that was varied for the different measurement series.

For all experiments the same rod (internal diameter $Ød_i$ = 25 mm, outer diameter $Ød_o$ = 35 mm, internal length l = 500 mm) was used.

3.4. Temperature measurements

Among the 39 thermocouples only the averaged fluid temperatures are presented in Fig. 3 (a-e), since they are the most meaningful with regard to the fluid's heat transfer capability. Unfortunately, no results for a liquid fraction of 40% at 250 W can be presented because the temperatures of the rest rig exceeded the allowable maximum.

Fig. 3 (a-e) shows the lowest temperatures in the upper region of the rod for a liquid volume fraction of 25% for any heat input. This means, that the optimum heat transfer occurs for a liquid-to-gas ratio of 1:3 independent of the temperature in the range of 25 °C to 100 °C. The temperatures in the lower part of the rod rise with increasing charge, indicating a worse heat rejection from the fluid to the cooled wall.

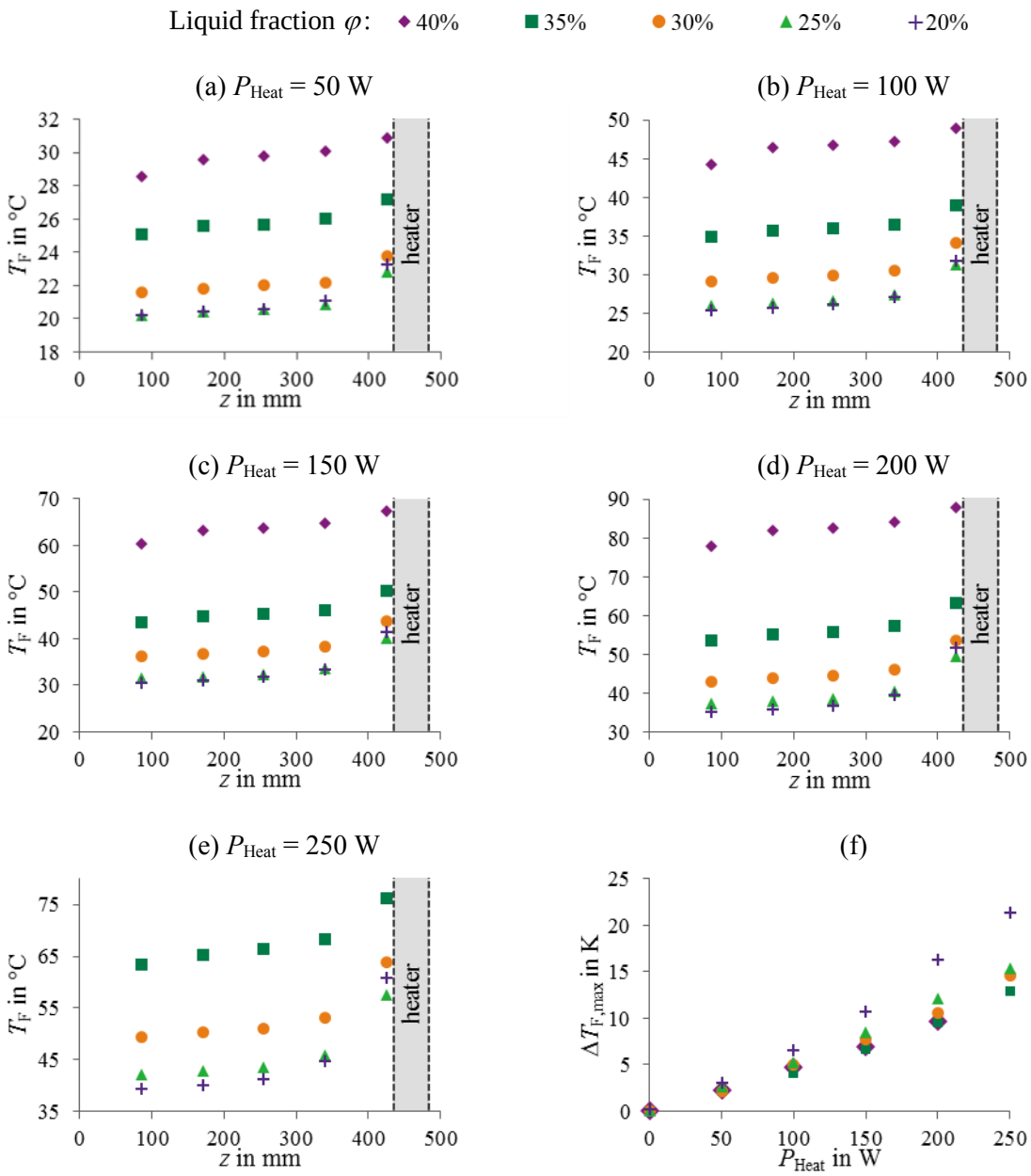

Figure 3. Averaged fluid temperatures of the steady-state period (a-e) and maximum fluid temperature differences (f) for varying liquid fractions and heat inputs

In Fig. 3 (f) the maximum temperature difference ($\Delta T_{F,max} = T_{F,1}$-$T_{F,5}$) are presented for every measurement. This gives access to the thermal resistance within the fluid. It can be seen that the highest temperature differences occur for the smallest liquid fraction of 20% which is mostly caused by large gradients in the upper section of the rod. This can be explained based on the too small liquid charge which only insufficiently reaches the upper parts of the rod. The smallest difference and by that the lowest thermal resistance between the upper- and undermost fluid TC is given for the liquid fractions of 35% and 40% which do not differ significantly. In addition, these values deviate also only slightly from the measurement run with the optimal overall heat transfer (ε = 25%). This leads to the assumption that for the examined configurations, the heat transfer within the fluid plays only a minor role compared to the heat transfer from the fluid to the wall at the cold end.

3.5. Thermal simulation

In accordance with the simulation procedure presented in a previous work[6], the temperature field for all measurements was calculated. For this, the measured temperatures from the rod's end cap, from within the insulation layers and from the crosshead are used as boundary conditions and the thermal behaviour of the filling is varied in an iterative procedure to match the fluid and the wall temperatures of the simulation with the experimental results. The simulation based on the finite element method is used to derive the axial heat flux of the fluid cross section at medium rod height as a quantitative heat transfer measure (see Tab. 1).

Table 1. Axial heat flux $\left|\hat{\dot{q}}_{\mathrm{z}}\right|$ in $\frac{\mathrm{W}}{\mathrm{cm}^2}$ and axial heat flow $\left|\dot{Q}_{\mathrm{z}}\right|$ in W (in parentheses) from the simulation for the fluid cross section at medium rod height (z = 0.25 m)

		Liquid volume fraction ε in %					Maximum axial heat flux $\left\|\hat{\dot{q}}_{\mathrm{z,max}}\right\|$ in $\frac{\mathrm{W}}{\mathrm{cm}^2}$
		20	25	30	35	40	
Heat input P_{Heat} in W	50	8.5 (41.7)	8.6 (42.2)	8.5 (41.7)	7.4 (36.3)	6.8 (33.4)	10.2
	100	16.3 (80.0)	16.5 (81.0)	16.2 (79.5)	15.3 (75.1)	13.4 (65.8)	20.4
	150	24.2 (118.8)	24.4 (119.8)	23.9 (117.3)	22.6 (110.9)	20.4 (100.1)	30.6
	200	31.9 (156.6)	32.2 (158.1)	31.4 (154.1)	30.0 (147.3)	24.7 (121.2)	40.7
	250	40.7 (199.8)	40.8 (200.3)	40.1 (196.8)	37.8 (185.6)	-	50.9

The values for the axial heat flux in Tab. 1 show that ca. 50 to 85% of the applied head load could be transferred through the rod. For the highest heat input (250 W) and the optimal liquid fraction (25%) about 220 W have been transferred through the fluid's cross section in axial direction, which corresponds to a temperature gradient $\Delta T/\Delta z$ of 45 K/m between the upper- and undermost FT. Though this is even a small temperature gradient in comparison to real applications, these results show that the ICRC can significantly contribute to reject heat from the packing and from the cylinder area.

3.6. Pressure measurements

For the investigation of fluid mechanical processes the pressure signals are shown in Fig. 4 for a heat input of 100 W and for n = 500 min^{-1}. On the left hand side the original signals of all 3 pressure sensors are shown for 10 crank turns. In a first step, these data was reduced to one representative period by averaging all pressure values related to the same crank angle value. That means, that *e. g.* exactly all values that correspond to the TDC position (0°, 360°, etc.) are averaged to one final value. In a second step, this period is processed by a rolling window (rolling average) analysis with a window width of 800 data points and window type "triang". This is done in order to remove small fluctuations for obtaining *e. g.* comparable peak values. More information on the rolling window processing, which has been executed via the Python package "pandas" can be found in [9]. The results of both data reducing steps can be seen in the diagrams at the right hand site of Fig. 4 where the index end "per" represents the period averaged time series and "per win" represents the time series after both processing steps (only shown for the p_{b} sensor).

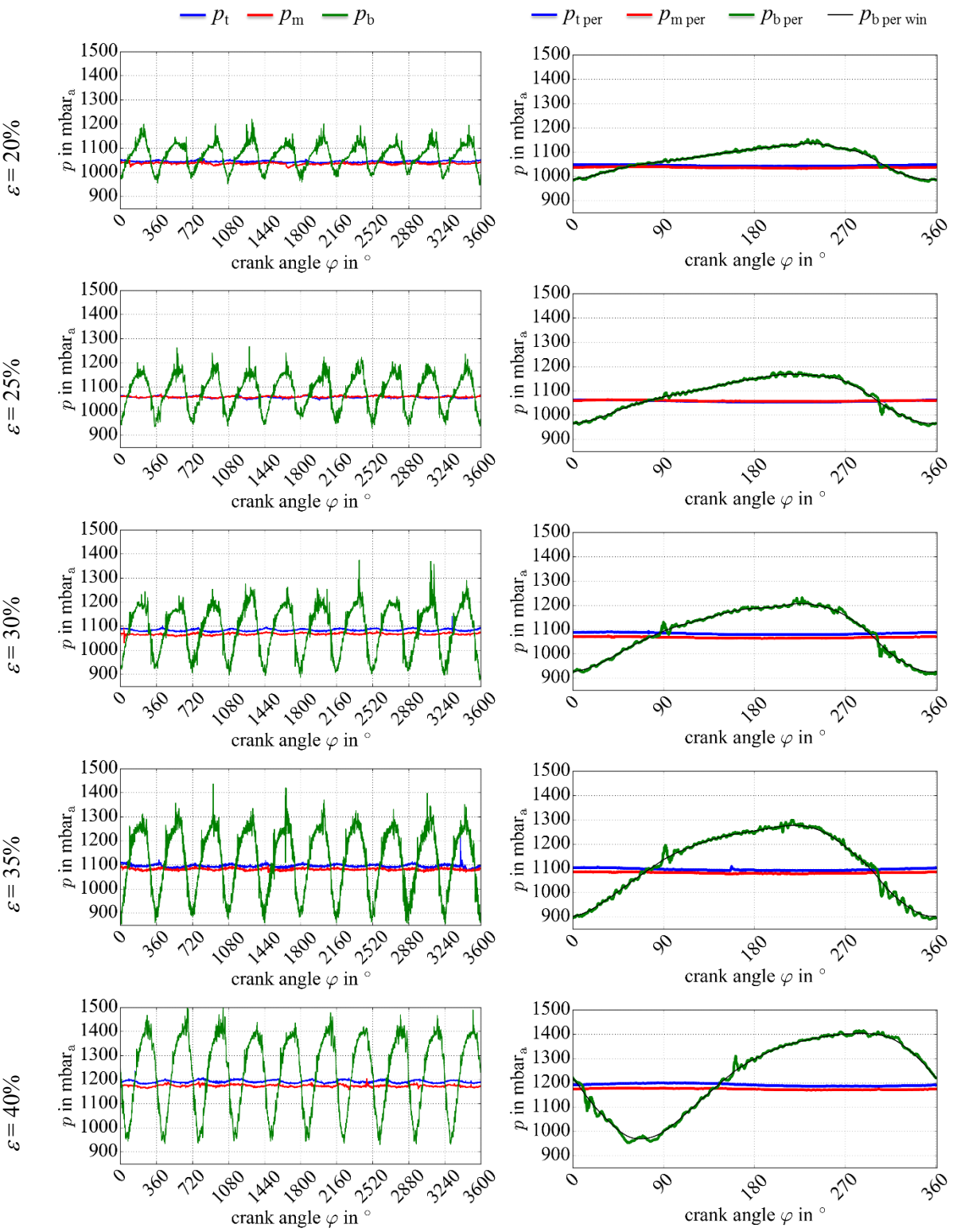

Figure 4. Original pressure signals (left) and processed pressure signals (right) (P_{Heat} = 100 W, n = 500 min^{-1}).

Fig. 4 shows that the pressure sensors at middle height (p_m) and at the top end of the rod (p_t) show only small fluctuations over time. Particularly, p_t happens to experience almost no liquid contact since

no pressure peak compared to the values of the pressure sensor at the bottom of the cavity (p_b) is visible. Hence, p_t presumably show just the change of volume for the gaseous phase in the upper part of the rod which is quiet small. This is not surprising, if one assumes both phases to be a continuum of which the liquid one is not compressible, thus, almost no compression of the other (gaseous) phase can be excited. Equivalent and in-phase time series can be seen for p_m which also see little influence of the liquid phase. Since the temperature gradients of Fig. 3 indicate a wetting at the location of p_m this could be explained by minor flow components in radial direction. The slight difference of the mean values of both signals originates from temperature differences between both measuring positions.

Most interesting, the p_b signal provides the best insight into the flow characteristics of the liquid phase. Its time course is mainly determined by the periodical movement of the rod since the highest fluctuations correspond to the frequency of the reciprocating motion. So the flow of the liquid phase mainly follows the rod's motion. In contrast, the p_b curves differ from the sinusoidal motion of the rod with regard to the peaks. The minima matches with the TDC position (except for $\varepsilon = 40\%$), but the maxima are delayed and do not correspond with the BDC position ($\varphi = 180°$). However, all 10 periods of each measurement run have quiet similar characteristics in terms of frequency and extrema. They differ only with regard to minor temporal phenomena within each period, which supports the abovementioned period-averaging approach.

3.7. Interpretation of pressure signals

The obtained data, particularly for the lower pressure sensor, can be used to draw conclusions about the periodical liquid behaviour over one crank revolution. One approach is to approximate the liquid phase to exist in two forms: On the one hand a sump at the bottom end of the rod that more or less follows the rod's motion. And on the other hand a liquid film, which originates from liquid that leaves the sump and which mainly sticks to the rod's wall due to surface tension forces. The volumes of the sump and the film change over one crank revolution.

For the analysis of the sump behaviour, the p_b signal is divided into two intervals. The first one is the interval where the pressure values increase. In this period, the fluid sump has the tendency to move downwards with respect to the rod's motion, thus, creating a higher load for the pressure sensor. The second one is the rest of the period where the pressure is decreasing. This strain relief of the pressure sensor occurs when a part of the liquid sump shows the tendency to move upwards with respect to the rod's motion. Then, a liquid portion leaves the sump mainly as liquid film at the wall quiet similar to what is known as annular flow. Tab. 2 summarises the relevant data deduced from the processed pressure signals ($p_{b\ per\ win}$).

Table 2. Deduced data from the $p_{b\ per\ win}$ time series (P_{Heat} = 100 W, n = 500 min^{-1}).

	Liquid volume fraction ε in %				
	20	25	30	35	40
p_{max} in mbara	1136	1169	1208	1277	1404
p_{min} in mbara	987	966	925	902	969
$p_{peak\text{-}to\text{-}peak}$ in mbar	150	203	282	375	435
$\Delta\varphi_{incr}$ in °	242	220	231	222	219
$\Delta\varphi_{decr}$ in °	118	140	129	138	141
Δt_{incr} in ms	81	73	77	74	73
Δt_{decr} in ms	39	47	43	46	47

The peak-to-peak values for the $p_{b\ per\ win}$ time series from Tab. 2 increase with increasing liquid fraction almost linearly. These peak-to-peak values show that the sump height over one crank rotation is increasing with larger amounts of liquid, since a larger liquid sump is acting on the pressure transducer. This illustrates that not the entire liquid charge is forced to leave the sump end. With increasing overall liquid charge, those liquid portion, which does not transfer heat from the rod's upper

to its lower part, is getting larger. It just blocks the lower end of the cavity and degrades the heat rejection, there.

Tab. 2 also shows that the length of intervals for increasing pressure values Δt_{incr} is about 1.5 to 2.0 times longer than the intervals for decreasing pressure values. If one assumes the increasing pressure interval to be the time period in which the liquid film returns to the sump, this time interval represents the period in which heat is actually transported from the upper end to the lower end. If the main heat flow is provided by the liquid motion, which means that the heat transfer through the gas phase is negligible, this axial heat transfer can be stated as following:

$$\left|\dot{Q}_z\right| = \dot{m}_l * c_{p,l} * \Delta T \quad (1)$$

Where $\dot{m}_l$ is the liquid mass flow, $c_{p,l}$ is the specific heat capacity of the liquid (for isobaric change of state) and ΔT is the corresponding temperature difference. When applying this formula on the middle section of the rod, where an almost linear temperature gradient can be found between $T_{F,2}$ and $T_{F,4}$ (see Fig. 3), the necessary liquid mass flow can be calculated based on the simulated heat flow values taken from Tab. 1. For a first approximation, this mass flow is assumed to be constant over time. The corresponding mean velocity v_l to this mass flow is calculated according to:

$$v_l = \Delta z_{T2\text{-}T4}/\Delta t_{incr} \quad (2)$$

where $\Delta z_{T2\text{-}T4} = 170$ mm is the vertical distance between the fluid TCs 2 and 4. Making use of the liquid mass flow $\dot{m}_l$, the liquid density ρ_l, and the mean velocity v_l the liquid flow area can be expressed as:

$$A_l = \dot{m}_l/(\rho_l * v_l). \quad (3)$$

If the liquid mass flow is furthermore assumed to appear as rotationally symmetric annular flow (circular ring) the film thickness of the liquid film is given as:

$$\delta_l = 0.5 * \{Ød_i - [Ød_i^2 - (4A_l/\pi)]^{1/2}\}. \quad (4)$$

The resultant values for this calculation are summarized in Tab. 3 for a heat input of 100 W. All necessary fluid properties are provided by REFPROP[10].

Table 3. Deduced data from the $p_{b\ per\ win}$ time series ($P_{Heat} = 100$ W, $n = 500$ min^{-1}).

	Liquid volume fraction ε in %				
	20	25	30	35	40
$\dot{m}_l$ in g/s	53.5	73.9	79.9	94.5	73.9
v_l in m/s	2.1	2.3	2.2	2.3	2.3
A_l in mm²	25.4	31.9	36.4	41.4	32.0
δ_l in mm	0.3	0.4	0.5	0.5	0.4

4. Summary

To access the heat transfer capability of the ICRC, experimental results from a vertically reciprocating internally cooled rod, which is heated at its top end, were presented and the heat transfer was investigated. It could be shown that for a natural coolant used in previous studies[5] a liquid/gas volume ratio of 1:3 shows the best cooling effect for the temperature range of 25 °C to 100 °C. Temperature measurements in conjunction with a finite element simulation have been used to quantify the axial heat flux of the fluid's cross section. The results prove that the ICRC can significantly contribute to reject heat from the packing and cylinder area of process gas compressors through the reciprocating assembly. Pressure measurements conducted simultaneously serve to interpret the fluid mechanical processes of the fluid mixture and conclusions could be drawn about the distribution and the flow of the liquid phase.

5. Outlook

Since the pressure measurements provide only local insight, an accurate examination of the flow inside the hollow rod is difficult to achieve. Therefore, optical measurements would be a promising option to investigate the occurring fluid mechanical phenomena in a satisfying way. Moreover and based on such visual results, a model to predict the flow is needed for precise calculations of the heat transfer inside a reciprocating hollow rod.

References

[1] Adair R P *et al* 1972 *Instantaneous heat transfer to the cylinder wall in reciprocating compressors* International Compressor Engineering Conference at Purdue, West Lafayette, USA
[2] Brok S W *et al* 1984 *Modelling of cylinder heat transfer – large effort, little effect?* International Compressor Engineering Conference at Purdue, West Lafayette, USA
[3] Shiva Prasad B G 1998 *Heat Transfer in Reciprocating Compressors – A Review* International Compressor Engineering Conference at Purdue, West Lafayette, USA
[4] Thomas (née Hammer) C 2013 *Innenkühlung der Kolbenstange von trockenlaufenden Kolbenverdichtern* (Doctoral dissertation). Technische Universität Dresden, Germany
[5] Patent DE 10 2007 000 652 A1
[6] Klotsche K *et al* 2016 *Experimental and numerical investigation of the heat transfer inside a hollow piston rod* International Compressor Engineering Conference at Purdue, West Lafayette, USA
[7] Klotsche K *et al* 2016 *Experimental and numerical investigation of the heat transfer inside a hollow piston rod* 10th EFRC Conference, Düsseldorf, Germany
[8] Reay D, McGlen R, Kew P 2013 *Heat pipes: theory, design and applications* Butterworth-Heinemann
[9] McKinney W 2010 *Data Structures for Statistical Computing in Python* Python for Scientific Computing Conference, Austin, USA
[10] Lemmon E W, Huber M L, McLinden M O 2013 *NIST Standard Reference Database 23: Reference Fluid Thermodynamic and Transport Properties-REFPROP*, Version 9.1, National Institute of Standards and Technology, Standard Reference Data Program, Gaithersburg, USA